

# THE EFFECT OF ACTIVE NOISE CONTROL ON THE EFFECTIVE MATERIAL PROPERTIES

Jordan Cheer and Stephen Daley

*Institute of Sound and Vibration Research, University of Southampton, Highfield, Southampton, UK*  
*email: j.cheer@soton.ac.uk*

Active noise control has been used in a variety of applications where it is impractical to achieve significant levels of noise control using traditional passive noise control treatments, for example, at low frequencies. In recent years, a similar performance benefit has been gained through the use of acoustic metamaterials, which achieve levels of noise control performance that are not achievable with naturally occurring materials. The high levels of noise control performance are generally attributable to the dispersive properties of these metamaterials and, as such, their behaviour has generally been evaluated in terms of their effective material properties, such as the effective density and bulk modulus. It is well known that the performance of active noise control systems is also frequency dependent, however, the links between these two advanced noise control strategies have not been extensively investigated. Therefore, this paper presents an investigation into how active noise control systems implemented in a duct modify the effective material properties. This work, therefore, begins to make links between the behaviour of acoustic metamaterials and active noise control systems.

Keywords: Metamaterial, Active Noise Control, Effective Material Properties

---

## 1. Introduction

Active noise control is a well developed technology that has been applied in a variety of applications to control low frequency noise. For example, it has been applied in the automotive environment to control low frequency engine and road noise [1], in the maritime sector to achieve high levels of noise and vibration control performance [2, 3], in the aerospace sector [4, 5], in consumer audio applications such as headphones [6] and in the built environment [7]. The key benefit of active control systems over traditional passive techniques is their ability to achieve high levels of control within a lightweight and compact package compared to traditional passive control treatments. In addition, they are able to adapt to changes in the noise and the acoustic environment, and provide the ability to not only reduce the noise level but shape its characteristics to manipulate the sound quality [8].

An alternative approach to achieving high levels of noise control performance at low frequencies, which has received significant interest in recent years, is the design of acoustic metamaterials. These materials do not achieve their noise control performance through the properties of the material itself, but through the engineered sub-wavelength structure of the system [9]. For example, metamaterials have been designed to achieve band gaps, which are spectral ranges over which the transmission of sound is limited, by using periodically arranged arrays of locally resonant elements [10]. These elements can take on a range of different forms, but could, for instance, simply be an array of Helmholtz resonators [11, 12]. Acoustic metamaterials have been shown to be able to achieve high levels of noise control performance in a traditional sense, for example by limiting the transmission of sound,

but have also been used to achieve more novel sound field manipulation objectives, such as acoustic cloaking [13]. In these applications, acoustic metamaterials are designed to achieve specific effective material properties, such as anisotropic behaviour [13], or negative effective density and bulk modulus [14]. Although these controlled effective material properties have been achieved using passive metamaterial designs [13, 15], recent attention has begun to focus on active acoustic metamaterials, where it is possible to increase the bandwidth of control, overcome losses that are inherent in a passive system and allow the system to be tuned or adapted [9].

Although a number of different active acoustic metamaterials have been demonstrated, the methodology adopted in the design of these active acoustic metamaterials generally differs from that employed in traditional active noise control. Recent work, however, has demonstrated how a traditional feedforward active noise control strategy can be used to control the transmission, as well as the effective bulk modulus, using an array of active Helmholtz resonators [16]. Metamaterials have also recently been used to solve the acoustic cloaking problem by designing metamaterials with particular material properties, however, in [17] it has been demonstrated that this problem can instead be solved by using active control to minimise the scattered component of the sound field, rather than attempting to directly control the effective material properties.

The work presented in this paper aims to further investigate the links between traditional active noise control systems and acoustic metamaterials, by investigating the influence of active noise control systems on the effective material properties, which are the usual metrics used when designing acoustic metamaterials. This study will be conducted within the context of controlling the sound in an anechoically terminated duct. Although this is a well studied problem, with well known solutions, it provides a transparent mechanism for beginning to investigate how such an active noise control system affects the effective material properties. Section 2 describes a number of different approaches to active noise control in an anechoically terminated duct and Section 3 presents the results of a series of simulations into the effective material properties of the active noise control strategies. Finally, Section 4 presents the conclusions.

## 2. Active Noise Control in a Anechoically Terminated Duct

The active control of noise propagating in one-dimensional ducts has been well studied and the theoretical formulations are summarised in [18]. Although the majority of work in this area has pragmatically focused on directly controlling the downstream pressure or minimising the acoustic power in the duct, as summarised in [18], a number of studies have also considered directly manipulating the acoustic impedance in the duct [19, 20]. The aim of the present study is to understand how standard active noise control strategies modify the effective material properties and, therefore, the control problems will be formulated as in [18] to minimise the downstream pressure or minimise the total power in the duct. In each case, the influence of the control strategy on the effective material properties will then be investigated.

Figure 1 shows the setup of the system that will be simulated to investigate the different control strategies. From this figure it can be seen that the primary source is located at one end of an anechoically terminated duct and the active control unit, which may consist of a number of different secondary source configurations, is located at some distance along the duct. If the frequency range of interest is restricted to low frequencies, where the wavelength is much larger than the largest cross-sectional dimension of the duct, it can be assumed that only plane waves propagate and the pressure at a position  $x$  in the duct due to the primary source can then be expressed as

$$p_p(x) = \frac{\rho_0 c_0}{2S} q_p e^{-jk|x+L|}, \quad (1)$$

where  $\rho_0$  and  $c_0$  are the density and speed of sound in air,  $S$  is the cross-sectional area of the duct,  $q_p$  is the volume velocity of the primary source,  $k$  is the wavenumber,  $x$  is the coordinate position in the duct and  $L$  is the distance between the primary source and the front of the active control unit at  $x = 0$ .

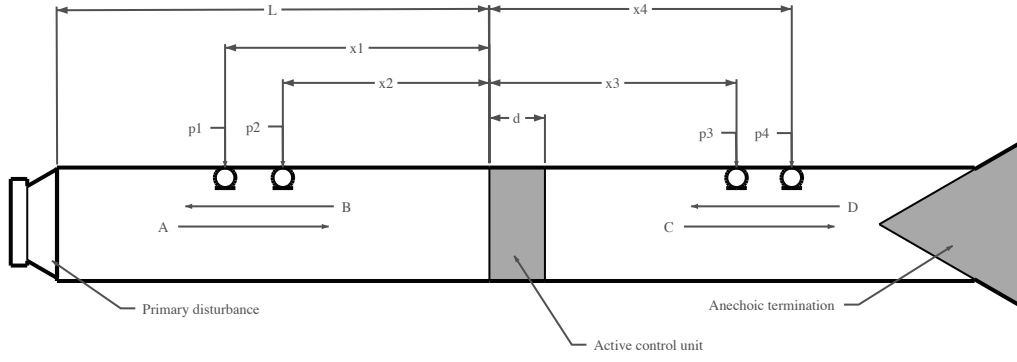


Figure 1: Diagram of the anechoically terminated duct setup with the primary disturbance loudspeaker, the four pressure evaluation positions and the location of the active control unit.

In active noise control, a secondary sound field is introduced in order to control the primary sound field. This process can be described by the superposition of the primary,  $p_p$ , and secondary,  $p_s$ , sound fields and can be expressed as

$$p(x) = p_p(x) + p_s(x). \quad (2)$$

In the following sections, a number of different approaches to specifying the secondary sound field are described.

## 2.1 Minimisation of the Downstream Pressure

In the first instance, a single monopole secondary source located at  $x = 0$  can be used to minimise the downstream pressure. In this case the objective of the secondary source can be expressed as

$$p(x) = 0, \quad x > 0. \quad (3)$$

Using eqs. (1) and (2) and the definition of the pressure due to a monopole plane wave secondary source, this objective can be expressed as

$$\frac{\rho_0 c_0}{2S} q_p e^{-jk(x+L)} + \frac{\rho_0 c_0}{2S} q_s e^{-jkx} = 0, \quad x > 0. \quad (4)$$

It is then straightforward to show that the optimal secondary source strength is given by [18]

$$q_s = -q_p e^{-jkL}. \quad (5)$$

The second active noise control configuration that will be considered, which is not considered directly in [18], is the case when a single dipole plane wave secondary source located at  $x = 0$  is used to minimise the downstream pressure. The sound pressure due to a plane wave dipole source can be expressed in terms of the downstream and upstream pressures as

$$p(x) = \frac{f}{2S} e^{-jk|x|}, \quad x > 0 \quad \text{and} \quad p(x) = -\frac{f}{2S} e^{-jk|x|}, \quad x < 0, \quad (6)$$

where  $f$  is the dipole force. The pressure downstream of the dipole secondary source can then be minimised by fulfilling the objective defined by eq. (3), which gives the net force required from the dipole secondary source as

$$f = -\rho_0 c_0 q_p e^{-jkL}. \quad (7)$$

This is clearly related to that required by the monopole secondary source in eq. (5), but it should be highlighted that the pressure produced upstream by the dipole source differs from that produced by a monopole secondary source.

Finally, control of the downstream pressure using two monopole secondary sources will be considered, as in [18]. In this case, one monopole secondary source is located at  $x = 0$  and the second monopole secondary source is located downstream from the first source at a distance  $d$ , as shown in Figure 1. The secondary sources are then driven to minimise the downstream pressure, whilst ensuring zero radiation in the upstream direction. Zero upstream radiation from the secondary sources is given by driving the first source with a volume velocity that is related to the second source by [18]

$$q_{s1} = -q_{s2}e^{-jkd}. \quad (8)$$

The total pressure can then be expressed through the superposition of the sound fields due to the primary and secondary sources, and the objective of minimising the downstream radiation can subsequently be expressed as

$$p(x) = \frac{\rho_0 c_0}{2S} q_p e^{-jk(x+L)} + \frac{\rho_0 c_0}{2S} q_{s2} e^{-jkx} (2j \cos(kd)) = 0, \quad x > d. \quad (9)$$

The optimum source strength for the secondary source located at  $x = d$  is then

$$q_{s2} = -q_p \frac{e^{-jkL}}{2j \cos(kd)}. \quad (10)$$

## 2.2 Minimisation of the Total Sound Power

Although minimisation of the downstream pressure is generally a practical approach to the control of sound propagating in a duct, there are a number of alternative approaches that may have benefits in certain circumstances or simply provide further insight into the mechanisms of control. One such alternative strategy is to minimise the total sound power in the duct, which attempts to minimise the radiation both upstream and downstream from the secondary source. The total sound power can be expressed for the primary and a single monopole secondary source as [18]

$$W = \frac{1}{2} \Re \left\{ \frac{\rho_0 c_0}{2S} (q_p + q_s e^{-jkL})^* q_p \right\} + \frac{1}{2} \Re \left\{ \frac{\rho_0 c_0}{2S} (q_s + q_p e^{-jkL})^* q_s \right\}. \quad (11)$$

This can be shown to provide a quadratic cost function and the optimal secondary source strength, which minimises the total acoustic power, is given by [18]

$$q_s = -\frac{1}{2} q_p \cos(kL). \quad (12)$$

As in the previous section, instead of using a single monopole secondary source to minimise the total sound power, it is interesting to consider the result when a dipole secondary source is employed, which has not previously been presented. If it is assumed that the sound field produced by the dipole source can be expressed in terms of two closely space monopole sources of equal and opposite source strength, then the total sound power can be expressed as

$$W = \frac{1}{2} \Re \left\{ \frac{\rho_0 c_0}{2S} (q_p - q_s e^{-jkL} + q_s e^{-jk(L+d)})^* q_p \right\} - \frac{1}{2} \Re \left\{ \frac{\rho_0 c_0}{2S} (q_s e^{-jkL} - q_s + q_p e^{-jkL})^* q_s \right\} \dots \\ + \frac{1}{2} \Re \left\{ \frac{\rho_0 c_0}{2S} (q_s - q_s e^{-jkL} + q_p e^{-jk(L+d)})^* q_s \right\}. \quad (13)$$

Through some manipulation, the optimal secondary source strength that minimises the total acoustic power is then given by

$$q_s = -\frac{1}{2} q_p \left( \frac{\cos(k(L+d)) - \cos(kL)}{1 - \cos(kd)} \right). \quad (14)$$

The total pressure field due to the dipole source can then be calculated according to eq. (6), where the force is given by  $f = j\omega\rho_0 q_s d$ .

Finally, the control of the total sound power using two independent monopole secondary sources is considered, which is again distinct from previous work. In this case, the vector of secondary source strengths,  $\mathbf{q}_s = [q_{s1}, q_{s2}]^T$ , which minimises the total sound power are given by

$$\mathbf{q}_s = - \left[ 2\mathbf{I} + \begin{bmatrix} 0 & 2\cos(kd) \\ 2\cos(kd) & 0 \end{bmatrix} \right]^{-1} \begin{bmatrix} 2q_p \cos(kL) \\ 2q_p \cos(k(L+d)) \end{bmatrix}. \quad (15)$$

### 2.3 Performance Metrics

In order to assess the performance of each of the active control strategies outlined above, the transmission, reflection and absorption coefficients, as well as the effective material properties have been calculated using the four microphone method. As described in [21], the pressures at the four microphones can be used to calculate the positive and negative travelling plane waves in the upstream and downstream sections of the duct, which are indicated by the coefficients  $A$  to  $D$  in Figure 1. The transmission, reflection and absorption coefficients can then be calculated respectively as

$$T = \frac{C}{A}, \quad R = \frac{B}{A} \quad \text{and} \quad \alpha = 1 - |R|^2.$$

The effective material properties of the active control unit can then be calculated using the transfer matrix method described in [21], which relates the pressures,  $P$ , and normal particle velocities,  $U$ , on either side of the active control unit via the transfer matrix,  $\mathbf{T}$ , as

$$\begin{bmatrix} P \\ U \end{bmatrix}_{x=0} = \begin{bmatrix} T_{11} & T_{12} \\ T_{21} & T_{22} \end{bmatrix} \begin{bmatrix} P \\ U \end{bmatrix}_{x=d}, \quad (16)$$

The elements of the transfer matrix can be calculated from the pressure and particle velocities at  $x = 0$  and  $x = d$ , which in turn can be calculated from the positive and negative travelling plane wave components [21]. The effective characteristic acoustic impedance can then be calculated as

$$z_{eff} = \rho_{eff} c_{eff} = \sqrt{T_{12}/T_{21}} \quad (17)$$

where  $\rho_{eff}$  and  $c_{eff}$  are the effective density and speed of sound through the active unit, and the effective wavenumber can be calculated as

$$k_{eff} = \frac{\omega}{c_{eff}} = \frac{1}{d} \cos^{-1} T_{11}, \quad (18)$$

where  $\omega$  is the angular frequency. The effective density and bulk modulus are then given as

$$\rho_{eff} = \frac{z_{eff}}{c_{eff}} = \frac{z_{eff} k_{eff}}{\omega} \quad \text{and} \quad B_{eff} = z_{eff} c_{eff} = \omega \frac{z_{eff}}{k_{eff}}. \quad (19)$$

## 3. Results

### 3.1 Minimisation of the Downstream Pressure

Using the geometry presented in Figure 1, the performance of the three active noise control strategies described in Section 2.1 have been calculated in terms of the transmission, reflection and absorption coefficients and the effective density and bulk modulus. These results are presented in Figures 2a and 2b. From Figure 2a it can be seen that the single monopole secondary source (blue lines) and the single dipole secondary source (red lines), achieve zero transmission, but perfect reflection and, therefore, zero absorption. It is insightful, however, to observe from Figure 2b that the effective density and bulk modulus of these two control strategies differ. The monopole secondary sources gives an

effective density and bulk modulus of zero, which correspond to the impedance of a pressure release boundary at the active unit. Conversely, for the dipole secondary source, although the transmission and reflection coefficients are identical to the single monopole case, the density and bulk modulus are very large (tending to infinity), and this corresponds to a rigid boundary at the active unit. Finally, it can be seen from Figure 2a that the pair of monopole secondary sources (black lines) achieves both zero transmission and reflection, and thus perfect absorption. The effective bulk modulus in this case is again close to zero, but the effective density is equal to the ambient density of air and this leads to a perfectly absorbing condition. Although, the results presented in Figures 2a and 2b are consistent with those already presented in the literature, observing the effective material properties directly provides a clear link to the concepts of acoustic metamaterials.

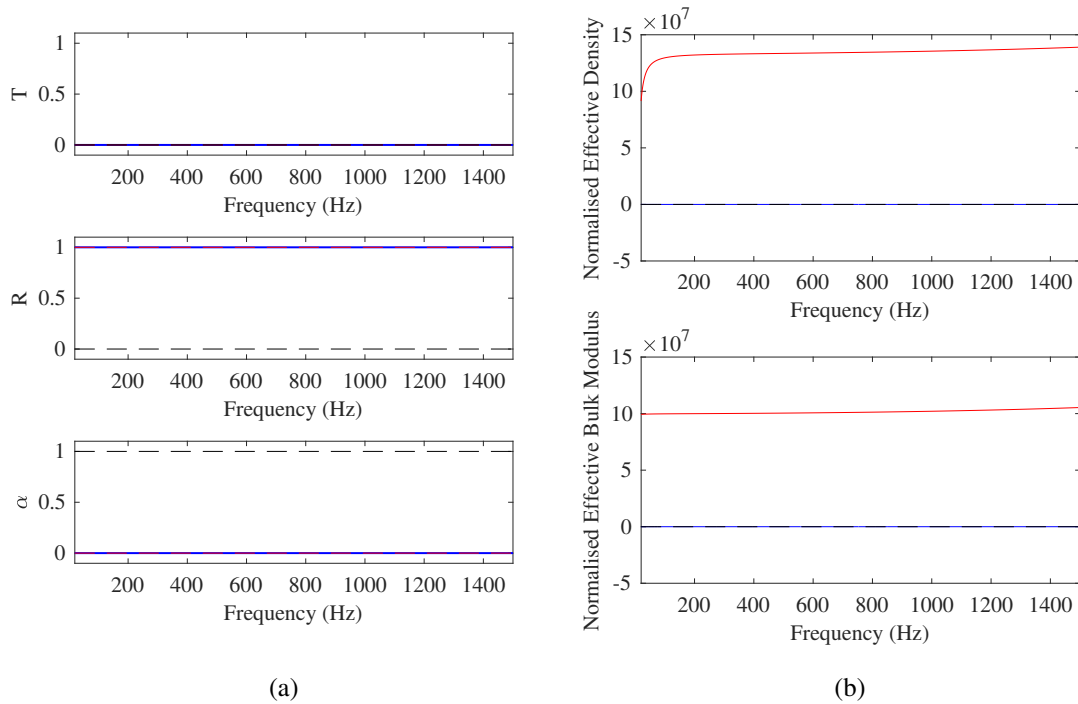


Figure 2: The performance of the active control systems optimised to minimise the downstream pressure using a single monopole secondary source (blue), a single dipole secondary source (red) and a pair of monopole secondary sources (black). (a) shows the transmission,  $T$ , reflection,  $R$ , and absorption coefficients,  $\alpha$ . (b) shows the effective density and bulk modulus normalised to the ambient values in air.

### 3.2 Minimisation of the Total Acoustic Power

An alternative approach to actively controlling the sound within a duct is to minimise the total sound power, as introduced in Section 2.2. This approach does not minimise the downstream pressure and, therefore, has received less attention in the literature; however, it leads to some interesting effective material properties that are linked to the objectives of many acoustic metamaterials. Figures 3a and 3b show the performance metrics for the three secondary source configurations, when they are driven to minimise the total sound power. From Figure 3a it can be seen from the blue and red lines that the single monopole and dipole secondary sources have transmission, reflection and absorption properties that are frequency dependent and fluctuate alternatively between perfect transmission and perfect reflection. In both cases, the total power in the system integrated over frequency is one half of the primary source power [18]. What is interesting, however, is that from Figure 3b it can be seen



that the monopole secondary source (blue lines) achieves bands of negative effective bulk modulus, and a normalised effective density of unity, whilst the dipole source (red lines) achieves bands of negative effective density, and a normalised effective bulk modulus of unity. These effective material properties are consistent with the resonant properties of acoustic metamaterials, in that a monopole resonance gives a negative effective bulk modulus and a dipole resonance gives a negative effective density [22]. This, therefore, makes an interesting link between active control mechanisms and the physics behind acoustic metamaterials.

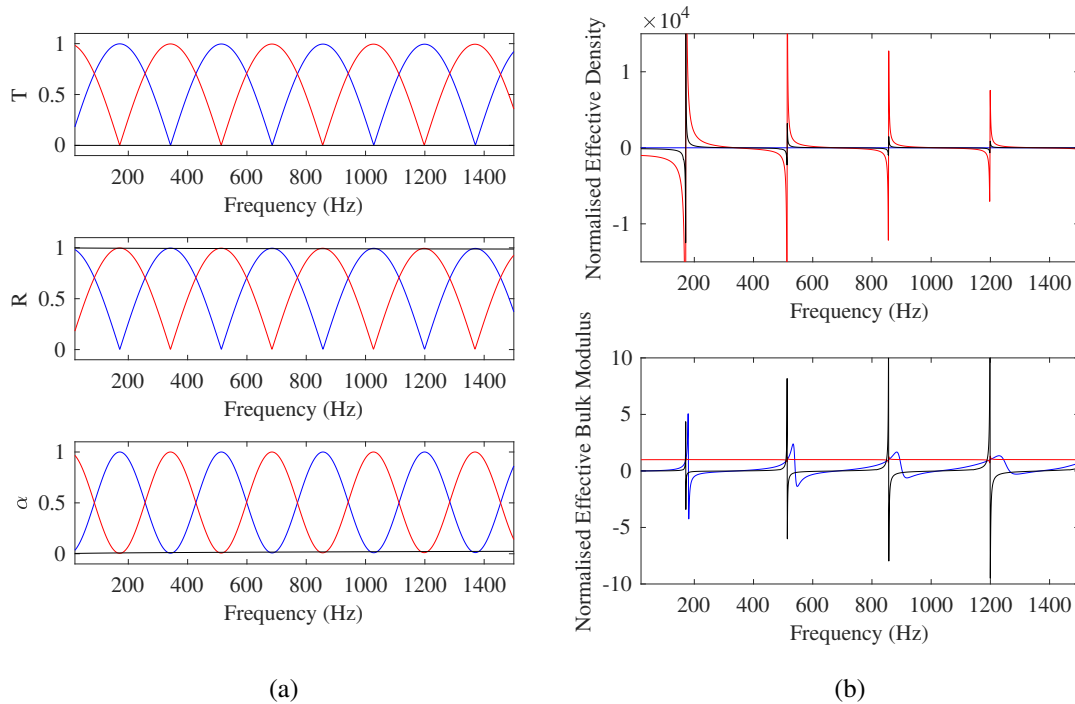


Figure 3: The performance of the active control systems optimised to minimise the total sound power using a single monopole secondary source (blue), a single dipole secondary source (red) and a pair of monopole secondary sources (black). (a) shows the transmission,  $T$ , reflection,  $R$ , and absorption coefficients,  $\alpha$ . (b) shows the effective density and bulk modulus normalised to the ambient values in air.

Finally, it can be seen from the black lines in Figure 3a that the pair of independent monopole secondary sources achieves zero transmission and perfect reflection, which is identical to the single monopole and dipole secondary source configurations optimised to minimise the downstream pressure in the previous section. However, from the black lines in Figure 3b it can be seen that this system achieves bands of both negative effective density and bulk modulus. Double negative metamaterials have been the focus of significant research due to their ability to control wave propagation and achieve negative refraction. Although such behaviour does not apply in the one-dimensional system considered here, the demonstration that these effective material properties are directly achievable using active control mechanisms provides significant insight into the design of future metamaterials.

## 4. Conclusions

The active control of sound in a one-dimensional duct has been well studied, however, limited attention has been paid to how these active systems influence the effective material properties. This has become of significant interest in recent years due to the surge in interest in acoustic metamaterials and their ability to induce unusual wave propagation. Therefore, this paper has investigated the effective

material properties of active noise control systems in a one-dimensional duct using monopole, dipole and pairs of monopole secondary sources to control the downstream pressure and total sound power. It has been shown that active control systems that minimise the total acoustic power lead to negative effective material properties and, therefore, may allow significant advancements in the realisation of active acoustic metamaterials.

## REFERENCES

1. Elliott, S. J., (2010), Active noise and vibration control in vehicles. Wang, X. (Ed.), *Vehicle Noise and Vibration Refinement*, pp. 235–251, Woodhead Publishing.
2. Daley, S., Zazas, I. and Hatonen, J. Harmonic control of a ‘smart spring’ machinery vibration isolation system, *Proceedings of the Institution of Mechanical Engineers, Part M: Journal of Engineering for the Maritime Environment*, **222** (2), 109–119, (2008).
3. Cheer, J. and Elliott, S. J. Active noise control of a diesel generator in a luxury yacht, *Applied Acoustics*, **105**, 209–214, (2016).
4. Elliott, S. J., Nelson, P. A., Stothers, I. M. and Boucher, C. In-flight experiments on the active control of propeller-induced cabin noise, *Journal of Sound and Vibration*, **140** (2), 219–238, (1990).
5. Lane, S. A., Clark, R. L. and Southward, S. C. Active control of low frequency modes in an aircraft fuselage using spatially weighted arrays, *Journal of Vibration and Acoustics – Transactions of the ASME*, **122**, 227–233, (2000).
6. Kuo, S. M., Mitra, S. and Gan, W.-S. Active noise control system for headphone applications, *IEEE Transactions on Control Systems Technology*, **14** (2), 331–335, (2006).
7. Bhan, L. and Woon-Seng, G. Active acoustic windows: Towards a quieter home, *IEEE Potentials*, **35** (1), 11–18, (2016).
8. Liu, F., Mills, J. K., Dong, M. and Gu, L. Active broadband sound quality control algorithm with accurate predefined sound pressure level, *Applied Acoustics*, **119**, 78–87, (2017).
9. Cummer, S. A., Christensen, J. and Alù, A. Controlling sound with acoustic metamaterials, *Nature Reviews Materials*, **1**, 16001, (2016).
10. Liu, Z., Zhang, X., Mao, Y., Zhu, Y., Yang, Z., Chan, C. and Sheng, P. Locally resonant sonic materials, *Science*, **289** (5485), 1734–1736, (2000).
11. Reynolds, M. and Daley, S. An active viscoelastic metamaterial for isolation applications, *Smart Materials and Structures*, **23** (4), 045030, (2014).
12. Ding, C.-L. and Zhao, X.-P. Multi-band and broadband acoustic metamaterial with resonant structures, *Journal of Physics D: Applied Physics*, **44** (21), 215402, (2011).
13. Popa, B.-I., Zigoneanu, L. and Cummer, S. A. Experimental acoustic ground cloak in air, *Physical review letters*, **106** (25), 253901, (2011).
14. Li, J. and Chan, C. Double-negative acoustic metamaterial, *Physical Review E*, **70** (5), 055602, (2004).
15. Lee, S. H., Park, C. M., Seo, Y. M., Wang, Z. G. and Kim, C. K. Acoustic metamaterial with negative modulus, *Journal of Physics: Condensed Matter*, **21** (17), 175704, (2009).
16. Cheer, J., Daley, S. and McCormick, C. Feedforward control of sound transmission using an active acoustic metamaterial, *Smart Materials and Structures*, pp. 1–24, (2016).
17. Cheer, J. Cancellation, reproduction, and cloaking using sound field control, *The Journal of the Acoustical Society of America*, **140** (4), 3312–3312, (2016).
18. Nelson, P. and Elliott, S. J., *Active Control of Sound*, Academic Press, London (1992).
19. Guicking, D. and Karcher, K. Active impedance control for one-dimensional sound, *ASME J. Vib., Acoust., Stress, Reliab. Des.*, **106**, 393–396, (1984).
20. Lacour, O., Galland, M. and Thenail, D. Preliminary experiments on noise reduction in cavities using active impedance changes, *Journal of sound and vibration*, **230** (1), 69–99, (2000).
21. Song, B. H. and Bolton, J. S. A transfer-matrix approach for estimating the characteristic impedance and wave numbers of limp and rigid porous materials, *The Journal of the Acoustical Society of America*, **107** (3), 1131–1152, (2000).
22. Haberman, M. R. and Guild, M. D. Acoustic metamaterials, *Physics Today*, **69** (6), 42–48, (2016).